

Size-Dependent Elastic State of Ellipsoidal Nano-Inclusions Incorporating Surface/Interface Tension

P. Sharma

e-mail: psharma@uh.edu

L. T. Wheeler

Department of Mechanical Engineering,
University of Houston,
Houston, TX 77204

Using a tensor virial method of moments, an approximate solution to the relaxed elastic state of embedded ellipsoidal inclusions is presented that incorporates surface/interface energies. The latter effects come into prominence at inclusion sizes in the nanometer range. Unlike the classical elastic case, the new results for ellipsoidal inclusions incorporating surface/interface tension are size-dependent and thus, at least partially, account for the size-effects in the elastic state of nano-inclusions. For the pure dilatation case, exceptionally simple expressions are derived. The present work is a generalization of a previous research that addresses simplified spherical inclusions. As an example, the present work allows us, in a straightforward closed-form manner, the study of effect of shape on the size-dependent strain state of an embedded quantum dot.

[DOI: 10.1115/1.2338052]

1 Introduction

The determination of elastic states of an embedded inclusion is of considerable importance in a wide variety of physical problems. In the classical elasticity context this problem was first solved rigorously by [1]. The latter work, both with and without modifications, has been employed to tackle a diverse set of problems: Localized thermal heating, residual strains, dislocation-induced plastic strains, phase transformations, overall or effective elastic, plastic and viscoplastic properties of composites, damage in heterogeneous materials, quantum dots, interconnect reliability, microstructural evolution, to name a few. The classical solution of an embedded inclusion neglects the presence of surface or interface energies and indeed, the effects of those are negligible except in the size range of tens of nanometers, where one contends with a significant surface-to-volume ratio. Clearly, the influence of surface/interface energies only extends to the nanoscale regime, as illustrated by various mechanical and optoelectronic applications such as nanostructures, nanocomposites, thin films, nanoelectronics, and quantum dots [2–10]. With this in mind, in a recent work, Sharma and Ganti [8] extended Eshelby's formalism to cover nano-inclusions by incorporating coupled bulk-surface elasticity. Explicit size-dependent expressions were presented for the elastic state of simplified spherical and circular shapes under radially symmetric loadings along with several illustrative applications. Sharma and Ganti [8] conclude that for shapes that admit a constant curvature (e.g., sphere, circular shape) and subjected to radial loadings, the elastic states are uniform. In the present work, we revisit the inclusion problem to address the more generalized ellipsoidal shape. We note here also several other works that have recently appeared addressing surface energy effects in inclusion problems: Duan et al. [11] generalized the work of Sharma and Ganti [8] to incorporate eigenstrains or loadings of arbitrary symmetry in spherical inhomogeneities. They find that interior stresses

and strains in spherical inhomogeneities are *nonuniform* if the eigenstrain or applied stresses are not radially symmetric. This conclusion is also affirmed independently by the work of Lim et al. [12]. Effective size-dependent properties of composites containing spherical inclusions have been addressed by Duan et al. [11] while Dingreville et al. [13] investigate the “effective” properties of nanoparticles, nanowires, and thin films.

Apart from the aforementioned works related to surface energy, in the classical elasticity context, extensive work has been done on the embedded inclusion problem and related issues. For the sake of conciseness, and given the existence of several readily available reviews on this topic, a detailed literature survey is avoided in this work. Wherever appropriate, relevant papers are cited contextually. The reader is referred to the following monographs, review articles, books and references therein: Mura [14], Nemat-Nasser and Hori [15], Markov and Preziosi [16], Weng et al. [17], Bilby et al. [18], Mura et al. [19], and Mura [20].

In Sec. 2, we discuss some preliminary concepts and issues related to surface/interface energies and inclusions. In Secs. 3 and 4, we employ the tensor virial method of moments to establish approximate solutions of various orders to the ellipsoidal nano-inclusion problem. Some simple expressions are deduced for the purely dilatational problem in Sec. 5. Numerical results and the application to quantum dots are presented in Sec. 6 followed with a summary and the major conclusions.

2 Preliminaries and Background

In this section, the mathematical preliminaries draw on the formulations of Gurtin and Murdoch [21], Murdoch [22], and Gurtin et al. [23]. In the context of inclusions, a reference to the words “surface” or “interface” is meant for the internal free surface of cavities or adjoining region of the solid inclusion and the surrounding matrix. In the present work, we shall use these words and their variants interchangeably.

Consider an arbitrarily shaped smooth interface between an embedded inclusion and surrounding host matrix, characterized by a unit normal \mathbf{n} . Let this interface be “attached” to the bulk (i.e., both inclusion and matrix) without slipping or any other discontinuity of displacements across it. This implies that we consider only a coherent interface. In contrast to the classical case where surface energies are neglected, we now require that the interface of the inclusion and the matrix be endowed with a deformation

Contributed by the Applied Mechanics Division of ASME for publication in the JOURNAL OF APPLIED MECHANICS. Manuscript received October 1, 2005; final manuscript received April 12, 2006. Review conducted by M. R. Begley. Discussion on the paper should be addressed to the Editor, Prof. Robert M. McMeeking, Journal of Applied Mechanics, Department of Mechanical and Environmental Engineering, University of California—Santa Barbara, Santa Barbara, CA 93106-5070, and will be accepted until four months after final publication of the paper itself in the ASME JOURNAL OF APPLIED MECHANICS.

dependent interfacial energy density, Γ . The interfacial or surface energy density is positive definite. This quantity is distinct from the bulk deformation dependent energy density due to the different coordination number of the surface/interface atoms, different bond lengths, angles and a different charge distribution [24].

Within the assumptions of infinitesimal deformation and a continuum field theory, the concept of surface stress and surface tension can be clarified by the (assumed *linearized*) relation between the interface/surface stress tensor, σ^s , and the deformation dependent surface energy, $\Gamma(\varepsilon^s)$

$$\sigma^s = \tau_o \mathbf{P}^s + \frac{\partial \Gamma}{\partial \varepsilon^s} \quad (1)$$

Where applicable, superscripts *B* and *S* indicate bulk and surface, respectively. Here, ε^s is the strain tensor for surfaces that will result from the projection of the conventional bulk strain tensor on to the tangent plane of the surface or interface while τ_o is the deformation independent surface/interface tension. The surface projection tensor, \mathbf{P}^s which maps tensor fields from bulk to surface and vice versa is defined as

$$\mathbf{P}^s = \mathbf{I} - \mathbf{n} \otimes \mathbf{n} \quad (2)$$

Here, “ \mathbf{I} ” is the identity tensor. Consider an arbitrary vector \mathbf{v} . The tensor or dyadic product \otimes extends two vectors into a second order tensor, i.e., in indicial notation, $A_{ij} = a_i b_j$. The surface gradient and surface divergence, then, take the following form [23]:

$$\nabla_s \mathbf{v} = \nabla \mathbf{v} \mathbf{P}^s \quad (3)$$

$$\text{div}_s(\mathbf{v}) = \text{Tr}(\nabla_s \mathbf{v})$$

Here we have also defined the surface gradient operator (∇_s) and the surface divergence (div_s). “Tr” indicates the trace operation. We shall employ both index and boldface notation as convenient. Unless otherwise stated, all tensors are referred to a Cartesian basis and isotropy is assumed throughout.

The equilibrium and isotropic constitutive equations of bulk elasticity are

$$\text{div } \sigma^B = 0 \quad (4a)$$

$$\sigma^B = \lambda \mathbf{I} \text{Tr}(\varepsilon) + 2\mu \varepsilon \quad (4b)$$

At the interface, the concept of surface or interface elasticity [21,23], ordinarily ignored in the classical formulation is introduced

$$[\sigma^B \cdot \mathbf{n}] + \text{div}_s \sigma^s = 0 \quad (5a)$$

$$\sigma^s = \tau_o \mathbf{P}^s + 2(\mu^s - \tau_o) \varepsilon^s + (\lambda^s + \tau_o) \text{Tr}(\varepsilon^s) \mathbf{P}^s \quad (5b)$$

Here, λ and μ are the Lamé constants for the isotropic bulk material. Isotropic interfaces or surfaces can be characterized by surface Lamé constants λ^s , μ^s , and surface tension, τ_o . The square brackets indicate a jump of the field quantities across the interface. It is to be noted that only certain strain components appear within the constitutive law for surfaces due to the 2×2 nature of the surface stress tensor (i.e., only the tangential projection of the strains on the interface are included consequently, $\mathbf{P}^s \cdot \mathbf{n} = \mathbf{0}$). In the absence of surface terms, Eq. (5a) reduce to the familiar normal traction continuity equations.

Thus, while the infinitesimal strain tensor in the bulk (both inclusion and matrix) is defined as usual in Eq. (6), the surface strains involve the use of projection tensor (Eq. (7))

$$\varepsilon = \frac{1}{2}(\nabla \mathbf{u} + \nabla \mathbf{u}^T) \quad (6)$$

$$\varepsilon^s = \frac{1}{2}(\mathbf{P}^s \nabla_s \mathbf{u} + \nabla_s \mathbf{u}^T \mathbf{P}^s) \quad (7)$$

Implicit in Eq. (7) is our assumption of a coherent interface. An incoherent interface requires additional measures of strain. The most generalized treatment of deformation measures that allows

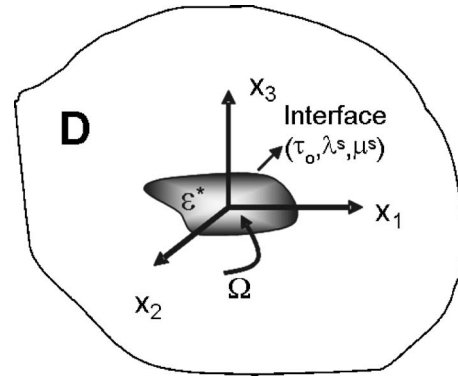


Fig. 1 Schematic of the problem

projections of jump in the displacement gradient (i.e., relative strain, twist, normal shear, tilt) and jumps in the normal and tangential displacement (stretch and slip) in addition to the coherent deformation considered in Eq. (7) has been addressed in detail by Gurtin et al. [23].

Consider a stress-free uniform transformation strain prescribed within the domain of the inclusion (Fig. 1). As per Mura's definition of an inclusion [14] we assume (*for the moment*) identical material properties for the inclusion and the matrix. The scenario where material properties differ is referred to as the inhomogeneity problem [14] and will be discussed in Sec. 6.

Sharma and Ganti [8] have derived the following general integral equation for arbitrary shaped inclusion linking the actual strain in the inclusion to the uniform transformation strain

$$\varepsilon = \mathbf{S} : \varepsilon^* + \text{sym} \left\{ \nabla_x \otimes \int_S \mathbf{G}^T(\mathbf{y} - \mathbf{x}) \cdot \text{div}_s \sigma^s(\mathbf{y}) dS_y \right\} \quad (8)$$

Here \mathbf{G} is the Green's tensor for isotropic classical elasticity [1]. ε^* is the so-called “eigenstrain” or a stress-free transformation strain such as due to for example, phase transformation, thermal expansion mismatch, lattice mismatch among others. The underlined term in Eq. (8) indicates the extra contributions due to surface/interface energy. \mathbf{S} is the classical size-independent Eshelby tensor (see [1], Appendix A and [14]). The notation, $\text{sym}\{\cdot\}$, represents the symmetric part of a second order tensor, \mathbf{A} , e.g., $\text{sym}\{\mathbf{A}\} = \frac{1}{2}(\mathbf{A} + \mathbf{A}^T)$. Some further details on Eshelby's tensor formalism are included in Appendix A for ready reference.

Further simplification of Eq. (8) is difficult without additional assumptions regarding inclusion shape. Equation (8) implicitly gives the modified Eshelby's tensor for inclusions incorporating surface energies. This relation is implicit since the surface stress depends on the surface strain, which in turn is the projection of the conventional strain (ε) on the tangent plane of the inclusion-matrix interface.

For the spherical shape, Eq. (8) can be explicitly re-written as [8]

$$\varepsilon = \mathbf{S} : \varepsilon^* - \frac{2(\lambda^s + \mu^s)}{3KR_o} (\mathbf{S} : \mathbf{I}) \text{Tr}(\mathbf{P}^s \varepsilon \mathbf{P}^s) - \frac{2\tau_o}{3KR_o} (\mathbf{S} : \mathbf{I}) \quad (9)$$

Here we note that for a sphere, curvature is the reciprocal of its radius, $\kappa = 1/R_o$, and K is the bulk modulus. To allow easy manipulation and in order to get analytical form of Eshelby tensor, it is necessary to resolve the fourth order tensors along the following basis: $\frac{1}{3} \delta_{ij} \delta_{kl}$ and $\frac{1}{2} (\delta_{ik} \delta_{jl} + \delta_{il} \delta_{jk}) - \frac{1}{3} \delta_{ij} \delta_{kl}$ (see for example, [25]). And using the spherical Eshelby tensor [14], Eq. (9) can be re-written (in spherical polar basis)

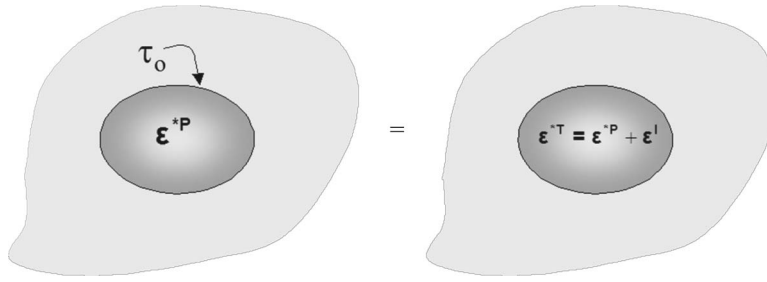


Fig. 2 Schematic of the solution

$$\varepsilon_{rr} = \varepsilon_{\theta\theta} = \varepsilon_{\phi\phi} = \frac{3K\varepsilon^* - 2\tau_0/R_0}{4\mu + 3K + 4(\lambda^s + \mu^s)/R_0} \quad (10)$$

A general feature of the integral Eq. (8) can be realized by noting that

$$\text{div}_s \sigma^s = \text{div}_s \{C^s P^s \varepsilon^P + \tau_0 P^s\} \quad (11)$$

The surface divergence of surface stress tensor can only be uniform if the classical “bulk” strain *as well as* the projection tensor is uniform over the inclusion surface. Consider the identity

$$\text{div}_s P^s = 2\kappa \mathbf{n} \quad (12)$$

Here κ is the mean curvature of the inclusion. For a general ellipsoid the curvature is nonuniform and varies depending upon the location at the surface. Thus, unlike for the spherical or circular shape, even for purely symmetric transformation strains such as pure dilation, we can expect a nonuniform strain state rendering perhaps impossible an exact solution of Eq. (8) for the general ellipsoidal shape.

3 Tensor Virial Method of Moments for Approximations to the Ellipsoidal Problem

The nonuniformity of the ellipsoidal curvature makes it difficult to solve for the elastic state via the implicit system of integral equations listed in Eq. (8). The direct use of the integral equation (8) is not very convenient for our purposes and thus in the remainder of this paper, based on some simplifying assumptions, we explore the so-called tensor virial method of moments [26] to deduce an approximate solution for an ellipsoidal inclusion undergoing a uniform transformation strain.

First, we only consider the effect of surface tension (i.e., τ_0) and ignore deformation dependent surface elasticity, for example, in the result of Eq. (10), the term $4(\lambda^s + \mu^s)/R_0$ would be discarded. This assumption is reasonable for small strains and indeed, as has been found in some technological applications, the deformation dependent surface elasticity effects can often be small compared to surface tension effect. Of course, in certain classes of problems, essential physics is lost by abandoning the deformation dependent surface elasticity (e.g., effective properties of nanocomposites, [8,11]; dislocation nucleation in *flat* nanosized thin films, [3]). However, for several problems of technological interest, consideration of τ_0 is sufficient. Note that the recent work of Yang [27] may require further clarification as he proposes that the effective size-dependent properties of nanocomposites depend on surface tension of inhomogeneities and fails to include the effect of surface elasticity which (according to us) is the sole contributor to the effect Yang purports to investigate. Since the effect of surface tension manifests itself as a residual type effect (i.e., independent of external loading), we can immediately employ Eshelby’s classic *gedanken* of cutting and welding operations [1] to put a physical perspective on the problem. Take the inclusion (containing a prescribed physical eigenstrain, say, a thermal expansion mismatch strain or that due to lattice mismatch) out of the matrix but with a surface tension equivalent to the interfacial tension of inclusion-matrix. From a classical perspective the inclusion

should relax to a strain equal to the physical eigenstrain. However, in the context of coupled surface-bulk elasticity, an additional strain ensues due to the presence of interfacial tension. Thus the total effective eigenstrain is equal to the superposition of the initial prescribed eigenstrain (due to a physical mechanism) and the strain state of an *isolated un-embedded* inclusion under the action of a surface tension. This is shown schematically in Fig. 2. Mathematically

$$\varepsilon^{*T}(\mathbf{x}) = \varepsilon^{*P}(\mathbf{x}, \text{physical cause}) + \varepsilon^I(\mathbf{x}, \tau_0, \kappa) \quad (13)$$

Here we have indicated the major functional dependence of each type of eigenstrain. The superscripts “T,” “P,” and “I” stand for “total,” “physical,” and “isolated” respectively. In summary, if we are able to evaluate ε^I , Eshelby’s classical tensor type concept can be employed to determine the elastic state of the inclusion incorporating surface energy, i.e.,

$$\varepsilon(\mathbf{x}) = \hat{S}(\mathbf{x}) : \varepsilon^{*T}(\mathbf{x}) \quad (14)$$

Here \hat{S} is an Eshelby tensor type integral operator which defaults to Eshelby’s classical tensor (S) for *uniform* eigenstrains. For an inhomogeneous eigenstrain, the actual strain is then determined by the action of the integral operator, \hat{S} . This distinction is necessary since even though (in this work) the physical eigenstrain is assumed to be (as often is) uniform, the contribution of surface tension is nonuniform, except in the case of a sphere and infinitely long circular cylindrical shape. Further details on \hat{S} are found in Appendix A. Note that the size dependence enters via the simulated eigenstrain, ε^I . For spherical and cylindrical shapes, the calculation of this strain is trivial. For example, in the spherical inclusion case, the isolated strain (in spherical polar basis) is merely $\varepsilon_{rr}^I = \varepsilon_{\theta\theta}^I = \varepsilon_{\phi\phi}^I = -2\tau_0/3KR_0$. Substituting this into (13) and using Eshelby’s tensor (Appendix A) reproduces Eqs. (9) and (10) and the result of Sharma and Ganti [8] provided that the surface elasticity constants, $\{\mu^s, \lambda^s\} \rightarrow 0$ in their formula, are set to zero which then also coincides with the result of Cahn and Larche [28].

For an ellipsoidal inclusion, even the isolated solution is not so trivial. We construct an approximate solution using the tensor virial method developed by Chandrasekhar [26,29].

Consider an isolated (i.e., un-embedded) triaxial ellipsoid made from the same material as the inclusion (Fig. 3). Further, let it

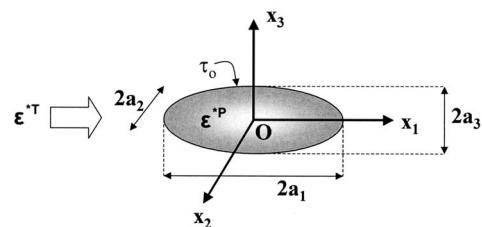


Fig. 3 Schematic of the problem for the isolated ellipsoidal particle under a surface tension

contain an eigenstrain identical to that of the inclusion, $\boldsymbol{\varepsilon}^{*P}$. Now, to incorporate surface energy (as per the discussion of the preceding paragraph), let the isolated ellipsoidal particle also be under the influence of a surface tension numerically equivalent to the interfacial tension of inclusion-matrix. A coordinate system with an origin at the ellipsoid centroid coincident with the principal axes of the ellipsoid (a_1, a_2, a_3) is adopted.

In the absence of any external body forces and in static equilibrium, the equation of motion for the isolated ellipsoidal particle can be written as

$$\text{div } \boldsymbol{\sigma}^I = 0 \quad (15a)$$

$$\boldsymbol{\sigma}^I = \mathbf{C}:\boldsymbol{\varepsilon}^I \quad (15b)$$

Where we note that $\boldsymbol{\varepsilon}^I$ can be found by simply inverting Eq. (15b). We take the first moment of Eq. (15a) to obtain

$$\int_V \mathbf{x}_i \frac{\partial \sigma_{ik}^I}{\partial \mathbf{x}_k} dV = \int_V \frac{\partial (\mathbf{x}_j \sigma_{ik}^I)}{\partial \mathbf{x}_k} dV - \int_V \sigma_{ij}^I dV = 0 \quad (16a)$$

$$\Rightarrow \int_S \mathbf{x}_j \sigma_{ik}^{I(-)} dS_k - \int_V \sigma_{ij}^I dV = 0 \quad (16b)$$

Gauss's theorem is used to obtain the surface integral in Eq. (16b). A superscript $(-)$ sign indicates that the referred quantity is applicable at distances infinitesimally close to the bounding surface but located in the interior. Since the inclusion is isolated, the $(+)$ quantities are identically zero. Recall that for uniform surface tension, the jump in the normal tractions is proportional to the surface tension (Eq. (5a)), i.e.,

$$[\boldsymbol{\sigma}^I \cdot \mathbf{n}] = -\boldsymbol{\sigma}^{I(-)} \cdot \mathbf{n} = -\tau_o \mathbf{n} \text{ div } \mathbf{n} \quad (17)$$

From which we obtain the relation

$$\int_V \sigma_{ij}^I dV = -\tau_o \int_S \mathbf{x}_j \text{ div } \mathbf{n} dS_i \quad (18)$$

Consistent with the notion of taking a first order moment, we assume that $\boldsymbol{\sigma}^I$ is uniform within the ellipsoidal particle. Then, as clearly apparent, Eq. (18) furnishes us a method to find the "average" strain of an isolated inclusion under the action of surface tension and eigenstrain via a (relatively) simpler surface integral on the right hand side. Note that, effectively, Eq. (18) approximates the nonuniform boundary condition at the inclusion-matrix interface in Eq. (5a) in an "average" sense. Implicit in this assumption is the notion that the average inclusion strain in the ellipsoidal inclusion is representative of the actual nonuniform strain that one would obtain from a rigorous solution of the integral equations in Eq. (8). Equation (18), which is the heart of the first moment approximation, is exact in three cases: (i) For inclusions with constant curvature, i.e., spherical and circular shape (ii) the trivial case when surface tension is absent, (iii) for large "inclusion" size where curvature is effectively negligible. Clearly, the first moment approximation is expected to be inaccurate when ellipsoidal aspect ratios become extreme, e.g., flat crack like inclusion, and as such should be avoided. Since we are constructing an approximation for an ellipsoid as the associated fields depart marginally from the uniform case (sphere), our solution is not expected to satisfy the two-dimensional asymptotic limit when the ellipsoid degenerates to a circular cylinder (for which also the exact analytical solutions are known). To approximate an elliptical cylinder, our analysis must be repeated in a two-dimensional framework (although in that case, complex analysis tools may be more efficient possibly leading to exact solutions).

Using a Lemma by Rosenkilde [30,31]—see Appendix B, the surface integral in Eq. (18) can be further simplified to

$$\tau_o \int_S \mathbf{x}_j \mathbf{n}_{k,k} dS_i = \tau_o \int_S (\delta_{ij} - \mathbf{n}_i \mathbf{n}_j) dS = 2\mathbf{M}_{ij} \quad (19)$$

Note that the rightmost integrand in Eq. (19) is just the surface projection tensor. The derivation of Eq. (19) and other ellipsoidal surface integrals involving higher order moments of $\text{div } \mathbf{n}$ are given in Appendix B. We can then write the surface contributed eigenstrain of the ellipsoidal inclusion in the following simple manner:

$$\boldsymbol{\varepsilon}^I = -\frac{2}{V}(\mathbf{C})^{-1}\mathbf{M} \quad (20)$$

The tensor \mathbf{M} tensor can be reduced to

$$M_{ii} = \pi(a_1 a_2 a_3)^2 \tau_o (A_j + A_k) \quad (i \neq j \neq k) \quad (21a)$$

$$A_i = \int_0^\infty \frac{dt}{\Delta(a_i^2 + t^2)}, \quad \Delta^2 = (a_1^2 + t^2)(a_2^2 + t^2)(a_3^2 + t^2) \quad (21b)$$

Summation convention has been suspended in Eq. (21). Our choice of coordinate system coincident with the principal axes of the ellipsoid and the ellipsoidal symmetry in general restrict non-trivial terms to only the diagonal ones. The A_i integrals are similar to the ones that appear in Eshelby's [1] classical work (but *not* the same). They are easily cast in terms of elliptical integrals

$$A_1 = \frac{\sin^2 \phi \cos^2 \theta F(\theta, \phi) + \cos^2 \phi E(\theta, \phi) - (a_3/a_2) \sin \phi \cos \phi}{a_1^3 a_2 \sin^3 \phi \cos^2 \theta}$$

$$A_2 = \frac{\cos^2 \theta F(\theta, \phi) - (a_3/a_2) E(\theta, \phi) + (a_3/a_2) \sin^2 \theta \sin \phi \cos \phi}{a_1 a_2^3 \sin^3 \phi \cos^2 \theta \sin^2 \theta} \quad (22)$$

$$A_3 = \frac{E(\theta, \phi)(a_3/a_2)^2 F(\theta, \phi)}{a_1 a_2 a_3^2 \sin^3 \phi \sin^2 \theta}$$

Here, the following ordering of semi-axes has been assumed, $a_1 > a_2 > a_3$. E and F are the incomplete elliptical integrals of the first and second kind, respectively

$$E(\theta, \phi) = \int_0^\phi \frac{d\varpi}{\sqrt{1 - \sin^2 \varpi \sin^2 \theta}}$$

$$F(\theta, \phi) = \int_0^\phi \sqrt{1 - \sin^2 \varpi \sin^2 \theta} d\varpi \quad (23)$$

$$\theta = \sin^{-1} \frac{a_1}{a_2} \sqrt{\frac{(a_2^2 - a_3^2)}{(a_1^2 - a_3^2)}}, \quad \phi = \sin^{-1} \frac{a_3}{a_1}$$

Equations (22) are obtained by substituting $t = a_3 \sin \varpi / \sqrt{\sin^2 \phi - \sin^2 \varpi}$ in Eq. (21).

Obviously, for simpler shapes such as spheres, circular cylinders and spheroids, these elliptical integrals (E and F) degenerate to well-known elementary expressions (e.g., [32]). The final (interior) strains and stresses of the embedded ellipsoidal inclusion can be conveniently expressed as

$$\boldsymbol{\varepsilon} = \mathbf{S}:\boldsymbol{\varepsilon}^{*T} = \mathbf{S}:\left\{\boldsymbol{\varepsilon}^{*P} - \frac{2}{V}\mathbf{C}^{-1}\mathbf{M}\right\}$$

$$\boldsymbol{\sigma} = \mathbf{C}:(\mathbf{S} - \mathbf{I}):\left\{\boldsymbol{\varepsilon}^{*P} - \frac{2}{V}\mathbf{C}^{-1}\mathbf{M}\right\} \quad (24)$$

Note that we have used the Eshelby tensor (\mathbf{S}), not the operator ($\hat{\mathbf{S}}$), since in the first moment approximation, the total eigenstrain is uniform.

4 Higher Order Virial Moments

In the previous section a first order virial moment of the equations of motion led to the approximation of uniform strain in the ellipsoidal particle under the influence of a surface tension and consequently uniform strain in the embedded inclusion. Successively higher order moments of the equations of motion can be taken to obtain more accurate approximations. To obtain a non-trivial set of self-sufficient equations, the desired strain must be a polynomial of degree one $m-1$ where m is the order of the moment, e.g., in the previous section, a first order moment was taken consistent with a uniform strain (zero order polynomial).

The equations of motion (Eq. (15a)) are now multiplied by $x_j x_m$ and integrated over the volume. Analogous to Eq. (16), we arrive at

$$\int_S x_j x_m \sigma_{ik}^{(-)} dS_k - \int_V (x_m \sigma_{ij}^j + x_j \sigma_{im}^j) dV = 0 \quad (25)$$

Consistent with the second order virial moment, we shall assume the isolated elastic state to be a polynomial of degree $(m-1)$, which in the present case is a linear function of position, i.e.,

$$\sigma_{ij}^j = \sigma_{ij}^2 = \sigma_{ij}^1 + a_{ijk} x_k \quad (26)$$

Here, the coefficients a_{ijk} are constants to be determined with the aid of Eq. (25). The first term in Eq. (26), σ_{ij}^1 , is determined (as in the preceding section) by means of the first order virial moment equation.

Straightforward manipulation yields

$$\int_V (\sigma_{ij}^1 x_m + \sigma_{im}^1 x_j) dV = -2(M_{ijm} + M_{imj}) \quad (27)$$

Where we have used (Appendix B)

$$\tau_o \int_S x_j x_k \operatorname{div} \mathbf{n} dS_i = 2M_{ijk} + 2M_{ikj} \quad (28a)$$

$$M_{ijk} = \frac{\tau_o}{2} \int_S (\delta_{ij} - n_i n_j) x_k dS \quad (28b)$$

The reduction to Eq. (28b) is important since it immediately allows us to note that the integrand is manifestly an odd function. The ellipsoidal shape possesses three planes of symmetry and consequently an odd function must integrate out to zero on its surface. Thus, the second order virial moment approximation degenerates to the first moment approximation of the previous section, i.e., $a_{ijk}=0$. This of course implies that the ‘‘average’’ strain computed in the previous section is correct up to (first) linear order. Thus, at least a third order moment (or a quadratic approximation in the strain) is required to introduce a nonuniform strain in the elastic solution of an isolated ellipsoidal particle (and hence embedded inclusion).

In closure of this section, we point out the evident fact that due to the lengthy and tedious expressions involved, implementation is somewhat inconvenient beyond the first order approximation.

5 A Purely Dilating Ellipsoidal Inclusion

For the pure dilatational case ($\varepsilon^{*P} = \varepsilon^P \mathbf{I}$), exceptionally simple expressions can be derived which we now proceed to outline. We only address the uniform strain approximation (i.e., first order virial moment). Consider Eq. (24) which provides the strain tensor for an embedded inclusion incorporating surface/interface energies via the second order tensor, \mathbf{M} . Taking trace on both sides we obtain

$$\operatorname{Tr}(\varepsilon) = \operatorname{Tr}(\mathbf{S}:\varepsilon^{*T}) = \operatorname{Tr}(\mathbf{S}:\varepsilon^{*P}) - \operatorname{Tr}\left\{\mathbf{S}:\frac{2}{V}\mathbf{C}^{-1}\mathbf{M}\right\} \quad (29)$$

At this point we appeal to a general result derived by Milgrom-Shtrikman [33] which specifies that the trace of classical Eshelby’s tensor is a constant for all shapes, i.e., in other words, the dilatation within an inclusion is independent of shape. Equation (29) then transforms to

$$\operatorname{Tr}(\varepsilon) = \left(\frac{1+\nu}{1-\nu}\right)\varepsilon^P - \operatorname{Tr}\left\{\frac{2}{V}\left[\frac{1}{2\mu}S_{ijpq}M_{pq} + \frac{2\mu-3K}{18\mu K}S_{ijmm}M_{qq}\right]\right\} \quad (30)$$

This can be further simplified to

$$\operatorname{Tr}(\varepsilon) = \underbrace{\left(\frac{1+\nu}{1-\nu}\right)\varepsilon^P}_{\text{Classical result: Milgrom Shtrikman Trace}} - \underbrace{\frac{2}{V}\left[\frac{1}{2\mu}S_{ijpq}M_{pq} + \frac{2\mu-3K}{18\mu K}\left(\frac{1+\nu}{1-\nu}\right)M_{qq}\right]}_{\text{Shape and size-dependent results}} \quad (31)$$

The first term in Eq. (31) is simply the Milgrom-Shtrikman [33] trace valid for all shapes and as apparent solely a function of Poisson ratio of the matrix. The second term which involves \mathbf{M} can be made more explicit by using Eq. (21a)

$$\operatorname{Tr}(\mathbf{M}) = 2\pi(a_1 a_2 a_3)^2 \tau_o (A_i + A_j + A_k) = \mathcal{A} \tau_o \quad (32)$$

where we have used the definition of surface area (\mathcal{A}). Further, decomposing, \mathbf{M} into a trace and trace-free part, i.e., $\mathbf{M} = \frac{1}{3} \operatorname{Tr}(\mathbf{M})\mathbf{I} + \mathbf{M}'$ final result then takes a simpler form

$$\operatorname{Tr}(\varepsilon) = \underbrace{\left(\frac{1+\nu}{1-\nu}\right)\varepsilon^P}_{\text{Classical}} - \underbrace{\frac{2\mathcal{A}\tau_o}{V} \frac{1}{9K} \left(\frac{1+\nu}{1-\nu}\right) - \frac{1}{2\mu V} S_{ijpq} M'_{pq}}_{\text{Shape and size-dependent results}} \quad (33)$$

\mathcal{A} for a triaxial ellipsoid is usually expressed as

$$\mathcal{A} = 2\pi c^2 + \frac{2\pi b}{\sqrt{a^2 - c^2}} [(a^2 - c^2)E(\theta) + c^2\theta] \quad (34)$$

$$\operatorname{sn}(\theta, k) = \sqrt{1 - \frac{c^2}{a^2}}; \quad k = \frac{a}{b} \sqrt{\frac{b^2 - c^2}{a^2 - c^2}}$$

Here E is the complete elliptical integral of the second kind and inversion of the Jacobi elliptic function sn is required. Volume is simply $(4\pi a_1 a_2 a_3)/3$. The form of our results presented in Eq. (33) is especially convenient in that one can judge the departure from ‘‘shape isotropy’’ (i.e., spherical shape) by the magnitude of \mathbf{M}' (which is identically zero for a sphere). One can verify (once again) that upon substituting $\mathcal{A}/V=3/R_0$ and $\mathbf{M}'=0$ the spherical inclusion result of Sharma and Ganti [8] is recovered provided one ignores the deformation dependent terms in their expression. The new results for dilatation depart from the classical Milgrom-Shtrikman trace since \mathcal{A}/V and \mathbf{M}' are both shape-dependent. Size-dependency, obviously, also enters through \mathbf{M}'/V and \mathcal{A}/V .

6 Numerical Results and Applications to Shape and Size Effects in Band Gap of Quantum Dots

The incorporation of surface size-effects in the inclusion problem extends all previous application areas of Eshelby’s inclusion problem to the nanoscale. The present solution, now also allows study of shape effects beyond trivial shapes such as spherical or circular.

In the previous sections, identical material properties were assumed for the matrix and the inclusion. The differing elastic constants can be taken care of easily through Eshelby’s equivalent

Table 1 Properties used in numerical calculations

Property	Value
E_g^{∞} (eV)	1.94 [36]
$a_c + a_v$ (eV)	8.3 [36]
μ^M (GPa)	67
K^M (GPa)	102
K^H (GPa)	168
μ^H (GPa)	95
τ_o (J/m ²)	1.33

inclusion principle [1,14] when the eigenstrain is uniform (which is the case in our first order moment approximation). The equivalent inclusion principle was extended to the polynomial case by Sendeckyj [34] and thus can in principle be used for higher order moment approximations if desired although we hasten to point out that one must contend with yet more tedious expressions. First some general results are presented for *inclusions* followed by discussion of our results for quantum dots (*inhomogeneities*). The material parameters used for the quantum dot are summarized for convenience in Table 1 (Appendix C) and the physical eigenstrain is identified with the lattice mismatch between the quantum dot and the surrounding matrix. When discussing the applications to quantum dots, the differing properties of the inclusion and the matrix are taken into account using Eshelby's equivalent condition [1,14]

$$\begin{aligned} & \mathbf{C}^I \left[\mathbf{S} : \left(\boldsymbol{\varepsilon}^f + \boldsymbol{\varepsilon}^p - \frac{2}{V} (\mathbf{C}^I)^{-1} \mathbf{M} \right) - \left(\boldsymbol{\varepsilon}^p - \frac{2}{V} (\mathbf{C}^I)^{-1} \mathbf{M} \right) \right] \\ &= \mathbf{C}^M \left[\mathbf{S} : \left(\boldsymbol{\varepsilon}^f + \boldsymbol{\varepsilon}^p - \frac{2}{V} (\mathbf{C}^I)^{-1} \mathbf{M} \right) - \left(\boldsymbol{\varepsilon}^f + \boldsymbol{\varepsilon}^p - \frac{2}{V} (\mathbf{C}^I)^{-1} \mathbf{M} \right) \right] \end{aligned} \quad (35)$$

Here superscripts "I" and "M" indicate inhomogeneity and matrix, respectively. Equation (35) allows the determination of the fictitious eigenstrain, $\boldsymbol{\varepsilon}^f$, necessary to simulate the perturbation due to differing elastic constants of the matrix and the inhomogeneity.

6.1 General Results. In this section, we assume an inclusion undergoing a dilatational transformation strain. The effect of aspect ratio is studied by for both prolate ($a_1 = a_2 < a_3$) and oblate ($a_1 = a_2 > a_3$) geometry. Obviously our results are generic enough to tackle arbitrary ellipsoidal shapes; prolate and oblate cases are illustrated for a clearer insight into the shape effects.

Percentage deviation of the dilation from the spherical shape is shown for both prolate and oblate spheroids in Figs. 4(a)–4(d).

The results are plotted with respect to spheroid size (a_1) and aspect ratio ($r = a_3/a_1$). As can be appreciated the presence of surface tension renders the solution difficult to normalize hence for a better perspective, results are plotted for three different parametric values of the eigenstrain ε^{ps} (0.02, 0.04, and 0.06). In Figs. 4(a) and 4(b), three aspect ratios ($a_3/a_1 = r = 1.5, 2.5, 5$) are shown. Clearly, the effect of shape depends on both size and the magnitude of the physical eigenstrain. Keeping in mind the rather typical value of surface tension we chose (1.33 J/m²), consider the case of 2% mismatch strain which is about the norm for quantum dots/substrate systems grown using the Stranski-Krastanov method. For this case, even up to 2 nm inclusion size (at an aspect ratio of 5), the departure from the spherical shape (i.e., Milgrom-Shtrikman trace) is no more than 10%. Shape effects, however, get rapidly appreciable below 2 nm reaching almost 30% for an inclusion size of 1 nm. For larger mismatch eigenstrains (4% and 6%, respectively) the shape effects are indeed small barely reaching 6% deviation from the spherical shape at a mismatch of 6% and aspect ratio of 5. Figures 4(c) and 4(d) yields similar conclusions albeit different magnitudes.

There is a weak dependence of dilation on shape. One though does expect a quite a stronger effect on the principal strains which is illustrated for prolate inclusions in Fig. 5. It can be seen the strains inside the inclusion exhibit a strong nonhydrostatic effect. The equivalence of ε_{11} and ε_{22} is due to the obvious symmetry of the geometry.

6.2 Shape Effects in Quantum Dots. We next employ the present results to study the effect of quantum dot shape on the size-dependent strain and consequently its band gap. Quantum dots (QD) are of immense technological importance and are typi-

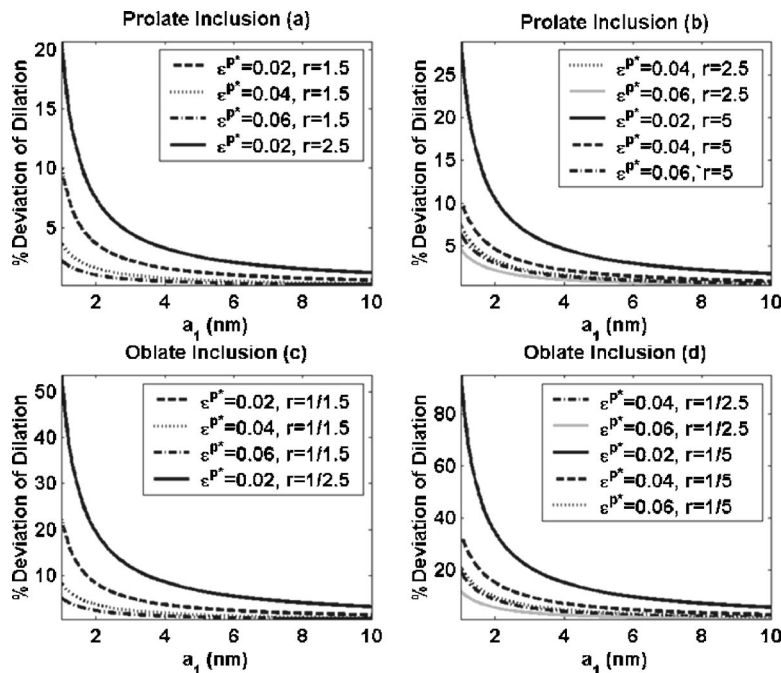


Fig. 4 (a)–(d): Effect of shape on size-dependent dilatation of ellipsoidal inclusions

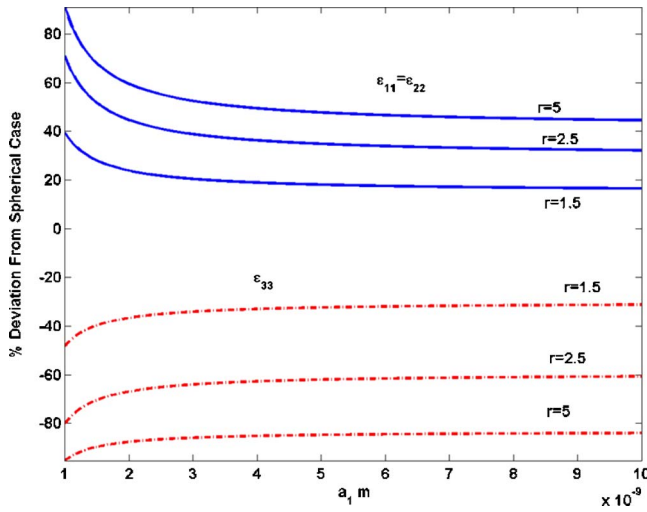


Fig. 5 Effect of shape on size-dependent principal strains of ellipsoidal inclusion, $a_1 = a_2 < a_3$, $r = a_3/a_1$. (a) $r=5$ (b) $r=2.5$ (c) $r=1.5$.

cally embedded in another semiconductor material with differing elastic constants and lattice parameter. The ensuing elastic relaxation within the QD is well known to impact their opto-electronic properties [35]. Acknowledging that quantum dots are often “fabricated” in the sub 10 nm regime, in our previous work [8], we reported significant shifts in band structure and optoelectronic properties for very small spherical quantum dots when one incorporates size-effects due to surface energies. While in most semiconductors the band structure is sensitive to all strain components, the major influence comes from the dilatation. From a classical point of view (based on classical elasticity theory), quantum dot optoelectronic properties have generally been considered relatively insensitive to shape (e.g., Andreev et al. [36])—although one can argue that this conclusion is a consequence of the several simplifying assumptions that typically made while proceeding to analytically calculate strain-band gap coupling. In light of Figs. 4 and 5 and the work of Sharma and Ganti [8] we can conclude that while size-effects due to surface effects may be significant at very small sizes, shapes effect is of secondary importance. A simple first order calculation can provide a numerical order to the shape effect¹

$$E^\infty + E^{\text{surf}}(R_o, a_3/a_1) + E^{\text{cl}} = E^\infty + (a_c + a_v)(\varepsilon_{kk} - \varepsilon_{kk}^{*T}) + O(\text{nondilatational terms}) \quad (36)$$

Where E^{surf} is the band gap shift due to the size and shape dependent contribution from surface energy induced strains while E^{cl} is the corresponding shift due to classical size-independent and (in the dilatational case) shape independent strain and finally E^∞ is the unstrained bulk crystal band gap. Here $(a_c + a_v)$ represents the dilatational deformation potential where, as indicated, we have ignored anisotropic terms both in elastic calculations as well as electronic calculations. Note that for the purposes of band structure calculations, the eigenstrain must be subtracted from the compatible strain. We take as an example, the technologically important In_{32}GaN quantum dot system embedded in a GaN matrix. We fix the size of the quantum dot at $a_1 = a_2 = 1$ nm to maximize the shape effect. We then obtain ΔE (net band gap shift due to shape at $a_1 = a_2 = 1$ nm, $r=1$, and $r=5$) of about 52 meV which is well beyond the strict tolerances for many optoelectronic devices [35]. At a more realistic quantum dot size of 5 nm, we obtain an error

¹A more rigorous calculation say using the multi-band k.p. method or tight binding approach is required for accurate electronic band structure calculation. For our purposes, the approximation in Eq. (36) is sufficient to illustrate our point.

of 7 meV which is small and most likely in the “noise” regime given the uncertainties in the determination of various other parameters of quantum dots (size, shape, material properties, etc.) that may have greater influence on the band structure than the variation in shape which we discuss.

7 Summary and Conclusions

In summary, we have extended a previous work on incorporation of surface/interface energies in the elastic state of inclusions to the ellipsoidal shape. In addition to the size dependency, the present formulation, also allows the possibility of a limited investigation of shape effects in various physical problems that typically employ the inclusion solution. Exact solution does not appear to be feasible for the problem addressed in this work and hence an approximate solution was constructed using the tensor virial method of moments. Although we employed only first order approximation in our numerical results, higher order approximations can be easily derived if such accuracy is required. In a sense, the present solution now incorporates shape effects into the scaling laws for inclusions that are valid at the nanoscale. In addition, exceptionally simple expressions were derived for the pure dilatational problem which is relevant for several physical applications. The discarding of deformation dependent surface elasticity prohibits use of the present results for calculations of effective properties of composites. The present work shares with its preceding companion article [8] much of the same limitations. For example, we have presented a completely isotropic formulation while interfacial/surface properties can be fairly anisotropic. In addition, we have assumed a perfectly coherent interface. In dealing with nano-inclusions it is important also to consider the degree of coherency, a complete investigation of which is left for future work.

Note added in proof. Our statement that residual stresses do not impact effective properties is only true under specific instances, however our statement regarding Ref. [27] stands. For further clarification on this issue, one may consult Huang and Sun [37]. The first author is grateful to Professor Z. P. Huang for educating him on this.

Acknowledgment

Help with plots from Xinyuan Zhang is gratefully acknowledged.

Appendix A: Eshelby’s Classical Tensor

In classical isotropic elasticity, the strain field for the inclusion problem is given by [1,14]

$$\varepsilon_{ij}(x) = \frac{1}{8\pi(1-\nu)} [\Psi_{kl,klj} - 2\nu\Phi_{kk,ij} - 2(1-\nu)(\Phi_{ik,kj} + \Phi_{jk,ki})] \quad (A1)$$

Where, ψ and Φ are bi-harmonic and harmonic potentials of the inclusion shape (Ω). They are given as

$$\Psi_{ij}(\mathbf{x}) = \varepsilon_{ij}^* \int_{\Omega} |\mathbf{x} - \mathbf{y}| d^3\mathbf{y} \quad (A2)$$

$$\Phi_{ij}(\mathbf{x}) = \varepsilon_{ij}^* \int_{\Omega} \frac{1}{|\mathbf{x} - \mathbf{y}|} d^3\mathbf{y} \quad (A3)$$

Equation (A1) can then be cast into the more familiar expression

$$\begin{aligned} \boldsymbol{\varepsilon}(\mathbf{x}) &= \mathbf{S}(\mathbf{x}) : \boldsymbol{\varepsilon}^* \quad \mathbf{x} \in \Omega \\ \boldsymbol{\varepsilon}(\mathbf{x}) &= \mathbf{D}(\mathbf{x}) : \boldsymbol{\varepsilon}^* \quad \mathbf{x} \notin \Omega \end{aligned} \quad (A4)$$

Mura’s book [14] contains detailed listing of \mathbf{S} and \mathbf{D} tensor for various inclusion shapes (spheres, cylinders, ellipsoids, and cuboids). When the eigenstrain is nonuniform, it must be brought

into the integral in which case, Eshelby's tensor is an integral operator.

Appendix B: Some Identities Related to Ellipsoidal Surface Integrals

In this Appendix, we derive some identities related to various order \mathbf{M} tensor. We simply illustrate the method by giving a derivation of M_{ijkl} which is not available in the literature [30,31].

Consider the following lemma [30,31] for an arbitrary tensor field \mathbf{A} :

$$\int_S \frac{\partial \mathbf{A}}{\partial x_l} dS_l = \int_S \frac{\partial \mathbf{A}}{\partial x_i} dS_i \quad (\text{B1})$$

In Eq. (B1) we set $\mathbf{A} = n_j x_j x_k x_m$. The left side of Eq. (B1) can then be expanded to

$$\int_S (\text{div } n) x_j x_k x_m + (n_j x_k x_m + n_k x_j x_m + n_m x_j x_k) dS_i \quad (\text{B2})$$

The right side of Eq. (B1) is written as

$$\int_S (\delta_{ij} x_k x_m + \delta_{ik} x_j x_m + \delta_{im} x_j x_k) dS \quad (\text{B3})$$

Equation (B3) can be used to derive the third order approximation if needed.

Appendix C: Material Properties for Numerical Calculations

The numerical values used are listed in Table 1. Further information on approximations of the interface elasticity constants is available from Sharma and Ganti [8]. For the quantum dot problem, all the properties in Table 1 and a dilatational physical eigenstrain corresponding to the lattice mismatch of 2% was used while for the inclusion problem, only $\mu^M K^M \tau_o$ were used.

References

- [1] Eshelby, J. D., 1957, "The Determination of the Elastic Field of an Ellipsoidal Inclusion and Related Problems," *Proc. R. Soc. London, Ser. A*, **241**, pp. 376–396.
- [2] Miller, R. E., and Shenoy, V. B., 2000, "Size-Dependent Elastic Properties of Nanosized Structural Elements," *Nanotechnology*, **11**(3), pp. 139–147.
- [3] Cammarata, R. C., Sieradzki, K., and Spaepen, F., 2000, "Simple Model for Interface Stresses With Application to Misfit Dislocation Generation in Epitaxial Thin Films," *J. Appl. Phys.*, **87**(3), pp. 1227–1234.
- [4] Kukta, R., Kouris, D., and Sieradzki, K., 2003, "Adatoms and Their Relation to Surface Stress," *J. Mech. Phys. Solids*, **51**(7), pp. 1243–1266.
- [5] Kouris, D., Peralta, A., and Sieradzki, K., 2000, "Surface Islands and Their Elastic Interaction With Adatoms," *Surf. Sci.*, **445**, pp. 420–429.
- [6] Sharma, P., and Ganti, S., 2002, "Interfacial Elasticity Corrections to the Elastic States of Quantum Dots," *Phys. Status Solidi B*, **234**, pp. R10–12.
- [7] Sharma, P., Ganti, S., and Bhate, N., 2003, "The Effect of Surfaces on the Size-Dependent Elastic State of (Nano) Inhomogeneities," *Appl. Phys. Lett.*, **82**, pp. 535–537.
- [8] Sharma, P., and Ganti, S., 2004, "Size-Dependent Eshelby's Tensor for Embedded Nano-Inclusions Incorporating Surface/Interface Energies," *J. Appl. Mech.*, **71**, p. 663.
- [9] He, L. H., Lim, C. W., and Wu, B. S., 2004, "A Continuum Model for Size-Dependent Deformation of Elastic Films of Nano-Scale Thickness," *Int. J. Solids Struct.*, **41**(3–4), pp. 847–857.
- [10] Lim, C. W., and He, L. H., 2004, "Size-Dependent Nonlinear Response of Thin Elastic Films With Nano-Scale Thickness," *Int. J. Mech. Sci.*, **46**(11), pp. 1715–1726.
- [11] Duan, H. L., Wang, J., Huang, Z. P., and Karihaloo, B. L., 2005, "Eshelby Formalism for Nano-Inhomogeneities," *Proc. R. Soc. London, Ser. A*, **461**(2062), pp. 3335–3353.
- [12] Lim, C. W., Li, Z. R., and He, L. H., 2005, "Size Dependent, Non-Uniform Elastic Field Inside a Nano-Scale Spherical Inclusion Due to Interface Stress," *Int. J. Solids Struct.* (to be published).
- [13] Dingreville, R., Qu, J., and Cherkaoui, M., 2005, "Surface Free Energy and its Effect on the Elastic Behavior of Nano-Sized Particles, Wires and Films," *J. Mech. Phys. Solids*, **53**(8), pp. 1827–1854.
- [14] Mura, T., 1987, *Micromechanics of Defects in Solids*, Martinus Nijhoff, Hague, Netherlands.
- [15] Nemat-Nasser, S., and Hori, M., 1999, *Micromechanics: Overall Properties of Heterogeneous Solids*, Elsevier Science, New York.
- [16] Markov, K., and Preziosi, L., 2000, *Heterogeneous Media: Micromechanics Modeling Methods and Simulations*, Birkhauser Verlag, Switzerland.
- [17] Weng, G. J., Taya, M., and Abe, H., eds, 1990, *Micromechanics and Inhomogeneity: The Toshio Mura Anniversary Volume*, Springer-Verlag, Berlin.
- [18] Bilby, B. A., Miller, K. J., and Willis, J. R., 1984, IUTAM/IFC/ICM Symposium on Fundamentals of Deformation and Fracture (Sheffield, England, 2–5 April 1984, Eshelby Memorial Symposium), Cambridge University Press, Cambridge, UK.
- [19] Mura, T., Shodja, H. M., and Hirose, Y., 1996, "Inclusion Problems," *Appl. Mech. Rev.*, **49**(10), pp. S118–S127.
- [20] Mura, T., 2000, "Some New Problems in the Micromechanics," *Mater. Sci. Eng., A*, **285**(1), pp. 224–228(5).
- [21] Gurtin, M. E., and Murdoch, A. I., 1975, "A Continuum Theory of Elastic Material Surfaces," *Arch. Ration. Mech. Anal.*, **59**, pp. 291–323.
- [22] Murdoch, A. I., 1976, "The Propagation and Fracture (Sheffield, England, 2–5 April 1984, Eshelby Memorial Symposium), Cambridge University Press, Cambridge, UK.
- [23] Gurtin, M. E., Weissmuller, J., and Larche, F., 1998, "The General Theory of Curved Deformable Interfaces in Solids at Equilibrium," *Philos. Mag. A*, **78**, pp. 1093–1109.
- [24] Ibach, H., 1997, "The Role of Surface Stress in Reconstruction, Epitaxial Growth and Stabilization of Mesoscopic Structures," *Surf. Sci. Rep.*, **29**(5–6), pp. 193–263.
- [25] Kleinert, H., 1989, *Gauge Field in Condensed Matter*, World Scientific, Singapore, Vol. 2.
- [26] Chandrasekhar, S., 1969, *Ellipsoidal Figures of Equilibrium*, Yale University Press, New Haven.
- [27] Yang, F., 2004, "Size-Dependent Effective Modulus of Elastic Composite Materials: Spherical Nanocavities at Dilute Concentrations," *J. Appl. Phys.*, **95**(7), pp. 3516–3520.
- [28] Cahn, J. W., and Larche, F., 1982, "Surface Stress and the Chemical Equilibrium of Small Crystals. II. Solid Particles Embedded in a Solid Matrix," *Acta Metall.*, **30**(1) pp. 51–56.
- [29] Chandrasekhar, S., 1965, "The Stability," *Proc. R. Soc. London*, **A286**, p. 1.
- [30] Rosenkilde, C. E., 1967a, "Surface-Energy Tensors," *J. Math. Phys.*, **8**(1), pp. 84–88.
- [31] Rosenkilde, C. E., 1967b, "Surface-Energy Tensors," *J. Math. Phys.*, **8**(1), pp. 88–97.
- [32] MacMillan, W. D., 1958, *The Theory of the Potential*, Dover, New York.
- [33] Milgrom, M., and Shtrikman, S., 1992, "The Energy of Inclusions in Linear Media Exact Shape-Independent Relations," *J. Mech. Phys. Solids*, **40**, pp. 927–937.
- [34] Sendecyk, G. P., 1967, "Ellipsoidal Inhomogeneity Problem," Ph.D. Dissertation, Northwestern University, Evanston, IL.
- [35] Singh, J., 1992, *Physics of Semiconductors and Their Heterostructures*, McGraw-Hill, New York.
- [36] Andreev, A. D., Downes, J. R., Faux, D. A., and O'Reilly, E. P., 1999, "Strain Distributions in Quantum Dots of Arbitrary Shape," *J. Appl. Phys.*, **86**(1), pp. 297–305.
- [37] Huang, Z. P., and Sun, L., 2006, "Size-Dependent Effective Properties of a Heterogeneous Material With Interface Energy Effect: From Finite Deformation Theory to Infinitesimal Strain Analysis," *Acta Mech.*, **190**, pp. 151–163.